

A Laboratory and Simulation Study of Condensate Gravity Drainage and its Implications for Field Development Strategies

M C Spearing, T P Fishlock, P I R Jones, B J Mead and J R Todd. AEA Technology, Winfrith, England

This paper was prepared for presentation at "Workshop on the Development of Gas Condensate Reservoirs" held at KFUPM, Dhahran, Saudi Arabia, 9 - 10 March, 1998.

Abstract

Development of gas condensate reservoirs via pressure depletion leads to condensation within the reservoir, and loss of valuable liquid components. Some laboratory measurements using X-ray in-situ saturation measurements indicate that the condensed liquid can drain under gravity. Better characterisation of condensate relative permeability under gravity drainage and simulation studies are required to investigate the implications for field development, and in particular to determine whether condensate drainage may permit improved recovery of the condensate liquids through suitably positioned production wells.

This paper first describes a laboratory study to quantify condensate relative permeability. Experimental methods for both the fluid handling and X-ray saturation monitoring of the fluid distribution in the vertically orientated core are discussed. The condensate saturation was developed in-situ by pressure depletion to maximum liquid dropout and saturation measurements were used to follow the extent of gravity drainage. Significant drainage was observed over a distance of 1m in only 10 days, demonstrating the potential for significant drainage with the time-scale of field developments. The core was subsequently flooded with equilibrium gas and liquid condensate was produced

The paper then briefly details the results of a scoping study to investigate the effect of various parameters on the drainage of liquid condensate. This was performed using a compositional simulator with simplified 1D and 2D reservoir models.

The simulation results show that the development of a large oil column through condensate liquid drainage is favoured by having a rich condensate, high vertical and horizontal permeability, and a significant condensate relative permeability at low condensate saturation. The presence of discontinuous shales may also be beneficial to condensate drainage. Some of the drained condensate can be captured using a suitably placed producer, raising the possibility of improved liquids recovery at little or no additional costs.

INTRODUCTION

Gas condensate reservoirs on the UKCS are usually developed by pressure depletion which leads to condensation within the reservoir and the loss of valuable liquid components. If the liquids are mobile they may accumulate at the bottom of the reservoir under the action of gravity drainage forming an oil rim that could be targeted later in field life.

The mobility of the condensate can be assessed in gravity drainage corefloods, however this is complicated by the fact that the mobile liquid may be trapped by capillary pressure end effects and not be produced at conditions of high gas/oil interfacial tension. Analysis of gravity drainage corefloods is aided by in-situ saturation monitoring, allowing end effects to be identified and relative permeabilities to be calculated from local changes in the liquid saturation, thus adding value to the experiment.

There has been a history of condensate drainage experiments performed by AEA Technology. Initially experiments were performed on a horizontal core. There was evidence that liquid condensate was produced during depressurisation but results were ambiguous. In the horizontal core it was unclear whether the mobile liquid would gravity segregate to the bottom of the core or be produced from the ends. For this reason a condensate experiment was conducted in a vertical orientation. The results from this second experiment showed that below a critical liquid saturation no oil was mobilised, but above this critical saturation oil was mobilised and produced by a drainage process. A low gas relative permeability was seen below the critical liquid saturation, and a higher value above the critical liquid saturation. This second experiment identified the need for in-situ saturation measurement to interpret the gravity drainage within the pore structure and to identify whether there was any capillary retention of the mobile oil at the outlet face.

The current experiment was performed with these objectives in mind. A coreflood was performed in which a single phase synthetic condensate was introduced into an outcrop sandstone above dew point pressure. The system pressure was reduced over a period of two days thus causing the liquid phase to condense to a volume of about 17% HCPV. The condensate liquid was allowed to drain for 16 days. In-situ saturation measurements were made during this period to monitor mobility of the liquid phase. At the end of this period the core was flooded with equilibrium gas and the in-situ saturation change monitored.

The experiment was performed at ambient temperature and the pressure corresponding to maximum liquid dropout. The objectives were to monitor gravity drainage, observe liquid mobility on gas flooding and identify capillary end effects, the

presence of which would adversely affect the measurement of gas relative permeability. This is a critical project parameter in determining reservoir productivity and therefore must be known if any reliability is to be placed on gas flooding results.

The in-situ saturation measurements were made using X-Ray in-situ saturation monitoring.

The first part of this paper reports on the experimental and theoretical techniques necessary to produce representative data. Subsequently the paper briefly details the results of a scoping study to investigate the effect of various parameters on the drainage of liquid condensate. This was performed using a compositional simulator with simplified 1D and 2D reservoir models. For reasons that will be explained later there was insufficient information to place useful limits on the condensate relative permeability curve and so the simulations were only intended as a scoping study.

RELATIVE PERMEABILITY LITERATURE REVIEW

Prediction of condensate drainage requires information on the appropriate condensate relative permeability. Conventional gas/oil relative permeabilities may not be appropriate because the oil phase is introduced in a different manner to the condensate situation where it is condensed in-situ, and for other reasons which will become apparent in this section. There has recently been a number of laboratory studies on condensate relative permeability which provide some relevant information. The experiments have been of two types, one to quantify factors which affect near-wellbore flow, necessary to predict well productivity, and the second to quantify gravity drainage. These measurements have revealed dependencies on the interfacial tension (σ), flow rate, and gravity (g). Researchers have suggested that the effects of individual variables can be combined through dependencies on the capillary number, N_c , and the Bond number, N_B . These may be defined as $N_c = \mu u / \sigma$, and $N_B = \Delta \rho g k / \sigma$, where μ is the gas viscosity, u is the Darcy velocity, $\Delta \rho$ is the difference in densities between condensate and gas, and k is the permeability. The two sets of results can be related if there is an equivalence in effects between N_c and N_B . Therefore, both types of experiment are considered here, and they are presented in historical order.

Danesh et al. [1] investigated the “critical condensate saturation” (CCS) in vertical Clashach and Berea sandstone cores. These cores were prepared to contain single-phase gas condensate and connate water. The cores were slowly depressurised by fluid extraction from the base and, at intervals, gas was injected into the top. The CCS was defined as that saturation at which gas injection gave a sustained flow of condensate. The CCS was about 8% for water saturations of 37 to 53%. However, injection before this saturation was reached gave a short period of condensate production, indicating condensate was mobile at lower saturations. Whilst these results do not provide sufficient information for predictive purposes, they do show that condensate may be mobile at low saturations in field developments. However, the results may be influenced by the high connate water saturation and the high Bond number, which may have been about 5×10^{-5} at the CCS, due to the low gas/oil interfacial tension.

In another set of experiments [2], a 1000 md vertical Clashach core was prepared to contain connate water and single-phase gas condensate. The pressure was reduced to form condensate in situ, and equilibrium gas and condensate injected to produce the desired condensate saturation. Injection was then stopped and the condensate allowed to drain under gravity. Four experiments were performed at different pressures, varying the gas/oil IFT over the range 0.047 to 0.21 mN/m. The corresponding range for the Bond number was 4 to 1×10^{-5} . For an IFT of 0.06 mN/m and an initial condensate saturation of 13%, almost half the condensate was recovered during 1000 hrs of drainage. Relative permeabilities deduced from the measurements showed the condensate curve to increase with decreasing gas/oil IFT, with much increased sensitivity below 0.06 mN/m. These results show the possibility of significant drainage within the field. However, the results may have been influenced by the high water saturation, which we have estimated at about 50%, and the unrepresentative manner in which the original condensate saturation was produced.

Danesh et al. [3] also investigated gas/condensate relative permeabilities at near-wellbore conditions in a series of core-flood experiments. A Berea core was prepared to contain single-phase gas condensate in the presence of connate water. A condensate saturation was then formed in situ by lowering the pressure below the dewpoint. Equilibrated gas and condensate fluids were then flowed through the core to give relative permeability data. Both the flowrate and the gas/oil IFT were varied. At the highest IFT studied (0.9 mN/m), condensate relative permeability appears to be independent of rate, although the gas relative permeability increases with rate. With a lower IFT of 0.14 mN/m, the relative permeability of both phases increases with rate. Overall, condensate relative permeability increases with decreasing IFT. The changes in relative permeability were deduced to depend on the capillary number. Fitting the k_{ro} value achieved at the highest oil saturation for an IFT of 0.14 mN/m to the Corey form used in the simulation studies (Equation (1)) yields a Corey exponent, n_o , in the range 2 to 3.

Boom et al. [4,5] performed a series of experiments to help elucidate near-wellbore behaviour. Most of the measurements were performed using a model system in which water represented the condensate and heptane the gas. Whilst this has many experimental advantages, the absence of a third phase, representing the connate water, complicates the application of results to real systems. Most of the measurements were performed in a centrifuge where the Bond number could be altered by using higher centrifugal acceleration and/or by adding isopropanol to the fluid system, to reduce the interfacial tension. The results indicated that the Bond number was the controlling parameter, rather than the IFT or the centrifugal acceleration. For a range of low Bond numbers, the “condensate” relative permeability showed only slight increase with increasing Bond number and the residual saturation was little affected. However, once a critical Bond number was reached, a further increase would lead to a significant reduction in the residual saturation and a slight steepening of the relative permeability curves. This critical value is typically in the range 10^{-5} to 10^{-4} . Additional measurements demonstrated the equivalence of Bond and capillary numbers in their effect on “condensate” relative permeability.

To summarise, laboratory data show that under suitable circumstances condensate can have a favourable relative permeability for gravity drainage which may justify use of Corey exponents as low as 2 or 3. The gas/oil interfacial tension is believed to be an important factor in the condensate relative permeability, possibly via a dependence on the Bond number. The condensate relative permeability may improve significantly as the Bond number rises above a critical value. This critical value is rock-dependent, and possibly in the range 10^{-5} to 10^{-4} . However, there are insufficient data at present to permit reliable estimation of condensate relative permeabilities for field appraisal studies and some laboratory results may have been influenced by water saturations which were higher than those typically found in the field.

EXPERIMENTAL DETAILS

This study was the first to be carried out using AEA Technology's new X-Ray scanning platform and was performed as much to test working practices with the scanner as to study condensate mobility under gravity drainage. Three phases would be present in the core (although it was hoped Swi would remain constant) and so both 2-phase (single energy) and 3-phase (dual energy) scans were performed. The 3-phase data would be subject to a follow on study if water was found to be mobile.

Description of the X-Ray Scanning Platform

The facility comprises a rigid gantry assembly which supports the vertical translational system of X-ray tube and detector. The experimental module is mounted on a platform which can be accurately positioned relative to the X-ray/detector system. This is shown schematically in Figure 1. The X-ray scanning platform enables high resolution saturation information to be generated and has the facility to operate in both single and dual energy modes. This allows 2-phase and 3-phase data to be collected. Sequences can be programmed in so that scanning can be automatically performed overnight if necessary. The computer controlled X-ray system provides a high photon flux, high stability and low ripple X-ray generation. The line array detector system allows a 0.5 mm resolution over a 512 mm field of view using 1024 detector elements. The detector head can be rotated by 90° allowing measurements to be taken in either X or Y planes. In this study, the scanner was set-up to take data horizontally at 30 positions up the vertical core with a slice height of 5mm and an interval of 3 cm between each scanning position, thus covering the complete core length.

Description of Condensate Module

The study was carried out using the condensate module which is a reservoir condition facility with maximum working conditions of 150°C and 10,000psi. The module was designed to be housed in a custom built oven, although the present experiment was performed outside of the oven to simplify scanning procedures. Methane and condensate were held in pistonless accumulators at test conditions with water as the driving medium. This allowed the process fluids to equilibrate with the water and thus prevent brine being stripped from the core during coreflooding. A vessel on the core outlet was provided to collect core effluent. The vessels were pressurised by means of water injection from a high pressure positive displacement pump and a second pump was

used to extract water from the outlet vessel to provide for a constant flow rate through the core. A carbon composite coreholder was used to allow the X-ray saturation measurements. A 40 bar overburden pressure applied to the core was maintained by an independent circuit using a nitrogen/water piston accumulator. The condensate module has a high temperature/high pressure PVT cell between the core and the outlet vessel for measurement of core effluent and condensate PVT characteristics. Rig pressures were monitored using five 0-700 barg pressure transducers and one 0-8 psi differential pressure transducer was used to measure the pressure drop across the core.

Synthetic Condensate Fluid: Hydrocarbon Composition

The same 5 component fluid composition as used in earlier AEAT studies was to be used in this experiment so that direct comparisons could be made. However, it was found by simulation that the previous fluid would actually be a volatile oil at 20°C . Therefore a new composition was designed that would be a condensate at room temperature (i.e. critical point below 20°C) and would show a sizeable amount of liquid dropout (approximately 25%). A series of PVT simulations were carried out starting with the composition of the fluid previously used, until a satisfactory composition was arrived at, see Table 1. A dopant with a high linear attenuation coefficient was also added to the fluid to aid the saturation monitoring - see later

The simulation showed this composition (without the dopant) to have a dew point of 215 barg at 20°C and a maximum liquid drop-out (MLD) of 24% at 186barg.

A constant composition expansion was performed in the PVT cell on the synthetic fluid prior to core flooding to check the characteristics of the fluid, as the effect of the dopant was unknown. The dropout characteristics are shown in Figure .2. Dewpoint was measured at 226.0 barg with a MLD of 21.3% at 130 barg. The liquid volume fraction was defined as the volume of oil as a percentage of the gas space in the PVT cell at dew point pressure. There was no peak to the liquid dropout curve measured; the liquid volume levelled off unlike the simulation which showed a peak at 186 barg.

Oil Phase Dopant Concentration

Calculations were performed to assess the scanning accuracy (standard error on repeat measurements) required to measure oil saturation to $\pm 1\%$ at the conditions of maximum liquid dropout. The calculations used mono-energetic linear attenuation coefficients for each fluid phase and so did not take into account the polychromatic nature of the X-ray beam. It was found that with no dopant, the scanning accuracy necessary was not attainable because of the relatively low density difference between the phases. Densities were 0.228 g/cm^3 and 0.435 g/cm^3 for the gas and liquid phases respectively with no dopant. Therefore a study of the effect of condensate liquid and water phase dopants on maximum permissible scanning error to achieve $\pm 1\%$ oil saturation (S_o) accuracy was performed. A 2-D plot of this is shown in Figure.3. The criterion used to which scans could be performed as a maximum practical accuracy was 0.01%. Figure 3 shows the combination of condensate liquid phase and water phase dopants that would meet this criterion. From a PVT point of view the quantity of oil phase dopant had

to be kept to a minimum. The minimum dopants still meeting the criterion was 25 wt% iododecane in decane or 9 wt% water phase dopant for the 3 phase system. The oil phase was chosen to be doped and this increased the linear attenuation coefficient of the equilibrium liquid by up to 2.2 times and that of the gas by 1.2 times over the undoped system.

X-Ray Calibration

The experiment was run as a 2-phase experiment with the connate water saturation assumed to remain constant. For a 2-phase experiment the system has to be calibrated with the hydrocarbon pore volume saturated with each of the two fluids to be measured at the conditions of the test.

Methane was used as an approximation for equilibrium condensate gas to cut down on the number of solvents floods which would be required at the end of the experiment if condensate gas was to be used for the gas calibration. The $S_{\text{methane}} = (1-S_{\text{wi}})$ calibration was performed at the start of the experiment prior to any characterisation measurements made on the condensate at the simulated pressure of maximum liquid dropout of 186 barg. It was later realised that this caused two unforeseen errors; firstly the use of methane was the main cause of saturation errors seen in the results; X-ray attenuation measurements in the PVT cell showed that there was up to 4% difference in the methane and condensate gas response which had a significant effect on measured saturations. Secondly, the simulated pressure of MLD (186 barg), at which the gas calibration was performed, did not equal the empirically found pressure of MLD (130 barg). The depressurisation (and oil calibration) was subsequently performed at 160 barg as a compromise which allowed a sizeable liquid dropout whilst not significantly affecting the linear attenuation coefficient of the gas from its value at 186barg.

The $S_{\text{condensate liquid}} = (1-S_{\text{wi}})$ could not be performed until after the equilibrium gas flood at which point the core was in the saturation state of S_{wi} , trapped equilibrium liquid and equilibrium gas. The core was first miscibly cleaned with pentane at 200barg, depressurised to 160 barg and flooded with equilibrium liquid, at which point the condensate liquid calibration took place.

An X-ray energy of 140 Kvp was used with 70 repeated measurements per position on the core for calibration and 15 repeated measurements per position on the core for data scans during the drainage. A 26 second exposure time was used for all measurements.

X-ray Normalisation

The X-ray beam is subject to long term drift, short term ripple and fluctuations on the individual detector elements. To combat this the raw X-ray data has to be normalised. Two forms of normalisation are used. A measurement on a piece of aluminium, positioned to the side of the core and sized to be of equal attenuation as the core/coreholder system, is taken as part of each core measurement, the aluminium covering a small number of detector elements. This is referenced to a measurement made at the start of the test to give an "edge" normalisation factor. At the start of a suite of measurements, once a day for example, a measurement is made on a piece of

aluminium covering the full 512mm fields of view. This referenced back to a measurement made at the start of the test to give "white" normalisation factors for each detector element. In this way all detector changes are allowed for.

Core Selection and Preparation

The core selected for the study was Clashach outcrop. A relatively high permeability core was chosen so that gravity drainage, if it was to occur, would be promoted. The core properties were as shown in Table 2

Depressurisation

The rig was set up so that the outlet vessel, PVT cell and the core were all on line to the condensate vessel. A CCE was then performed on the system as a whole by withdrawing water from the condensate vessel. The expansion was in the direction of bottom to top of the core. The liquid dropout observed and measured in the PVT cell (constant volume depletion, CVD) could be assumed to have also occurred in the core. The depressurisation took place in stages over a two day period and was at rates of approximately 7 - 15 barg / hour. Depressurisation was continued to 160 bar for reasons described in the earlier X-ray calibration section.

The gas/oil and oil/water interface levels in the PVT cell were noted during the depressurisation. No change in the liquid dropout volume was observed from 15 hours after the final pressure was reached to the end of the 16 day depressurisation period. Therefore the liquid was in equilibrium during this period. The liquid dropout at 160 barg measured in the PVT cell during the depressurisation was 15.5% (CVD).

Throughout the duration of the depressurisation, 2-phase and 3-phase scans were performed to monitor the drainage of liquid dropout. With each core scan, a single energy scan was performed on the PVT cell to monitor the attenuation of the liquid alone.

Equilibrium Gas Flood

Equilibrium gas from the condensate vessel was first pumped around the core by-pass and produced condensate liquid was measured. The PVT cell valves were arranged to act as a separator to check for water production.

The gas flood was performed in three stages, with scans performed at single HCPV intervals. The first HCPV throughput was at a rate of 100 ml/h, the second was at up to 200 ml/h and the third/fourth at rates up to 300 ml/h. Increasing rates were used so that further production would occur at each stage, giving the saturation monitoring a distinct saturation change to quantify.

Water Production

The maximum water production from the core amounted to 0.43ml (0.27%HCPV) from mass balance measurements. Although the results suggest that effectively no water was produced from the core, it is still possible that water redistributed within the core during the time since connate water was first established by nitrogen flooding. This is due to the change in the balance of capillary forces caused by the variations in interfacial tensions induced by the contact of the condensate

with the connate water. The 3-phase capability of the scanner could be used to monitor this.

EXPERIMENTAL RESULTS

Gravity Drainage

The drainage of condensate over a 16 day period is qualitatively demonstrated in Figure 4. In this figure, scans at 6 times after the core was depleted below dew point are shown. The images show detector array samples 57 to 63 and represent a 3cm strip down the centre of the core. The height of the core represented is from 12cm (top) to 87 cm (outlet). The colour scale runs from black, signifying 0% condensate liquid, to white signifying 100% liquid. The yellow signifies approximately 50% to 60% liquid. It can be seen that the height of the yellow increases up the core as time proceeds i.e. a build up of liquid condensate occurred. The build up in saturation seen in Figure 4 at the core outlet could not be due to water as the saturation change is too abrupt. The high IFT between water and condensate gas would cause a more dispersed saturation change if it were due to a water "end effect" caused by water movement.

Saturation data from nine scans are plotted in Figure 5 so that a quantitative assessment of the drainage can be made. The profiles show the saturation of detector array sample 61 only i.e. a 5mm strip down the centre of the core. Internal heating elements, not used but present in the coreholder affected the measurements at the edge of the core. For this reason a single sample from the centre of the core was used to represent the whole core. This approximation is only valid if the condensate saturation is uniform across the core. Data is only plotted from 24cm to 87cm down the core because calibration data from the first 23cm was invalidated by equilibrium gas inadvertently entering the core during the calibration flooding sequence to achieve $S_o = (1 - S_{wi})$. This occurred due to the practical problem of very little equilibrium oil available for the oil calibration at the end of the test. In the remaining 63cm it can be seen that the oil saturation in the body of the core gradually reduced over the drainage period and that a build-up occurred at the outlet. Drainage was still occurring after 16 days and so the system had not reached an equilibrium.

The average saturation in the core is plotted in Figure 6 for detector array sample 61. The saturation decreased from 30.5% to 26% during the drainage although no oil was produced into the PVT cell. This anomaly was taken as evidence that the assumption that the condensate saturation was uniform across the core was invalid. Inspection of Figure 4 shows that initially the condensate was not uniformly distributed within the core, but becomes more uniform from six days onwards. Figure 6 shows that the mass balance is approximately constant after 6 days.

The final average oil saturation of the core in Figure 6 was 26% HCPV. The maximum oil saturation however could only be 20% HCPV as measured by the CCE measurements. The in-situ saturations do not match the mass balance because methane was used as the gas calibration data whereas equilibrium condensate gas ideally should have been used. It has been shown analytically that a uniform 1% decrease in the gas calibration grey levels caused the scanner saturations to equal mass balance results. Comparison of the properties of methane and equilibrium gas in the PVT showed a 4% difference in the X-ray

attenuation. Due to the extra beam hardening effect of the core and coreholder over the PVT cell, it is likely that the attenuation difference between methane and equilibrium gas in the core would be near to the 1% required for the scanner saturations to equal mass balance results. The use of methane as the gas calibrant was intentional, as the extreme sensitivity of the scanner to the calibration gas was not envisaged prior to the experiment.

Gas Flood

From PVT mass balance measurements 9.1 mL of liquid condensate were produced from the core on equilibrium gas flooding. This was a reduction in the oil saturation of the core by 5.8 % HCPV. It is apparent that the high oil saturation at the outlet is reduced as the flood progresses. The gas flood saturation data for sample 61 are plotted in Figure 7. The liquid saturations in the main body of the core and at the core outlet progressively reduce with gas throughput. The average oil saturation fell from 31.1% HCPV to 25.2 % HCPV. This reduction of 5.9% HCPV compares very well with the 5.8% HCPV reduction measured from mass balance results.

Although the relative reduction in saturation was correct, the liquid saturation in the body of the core was greater during the gas flood than that at the end of the drainage, which cannot be the case as no further condensate entered the core on equilibrium gas flooding. The reason for the high liquid saturation in the body of the core during the gas flood remains unclear, but is possibly due to an artefact of the data normalisation process and/or the analysis of only of narrow region of the core.

3-Phase Data

Although water was found to be immobile, redistribution was a possibility. Therefore 3-phase X-ray calibrations were made so that the 3-phase scans could be analysed. Calibration for three phases requires scanning the core with 100% saturations of brine, condensate oil and condensate gas at 2 energies and at the pressure of the test. This would have required more equilibrium fluids than were available, so the attenuations of the fluids alone were measured in the PVT cell; calibrations were calculated from a 100% methane core scan adjusted for the measured attenuations of the equilibrium gas, condensate liquid and brine, and the different fluids thicknesses between the core and the PVT cell. However the 3-phase saturation data subsequently calculated was in error and no useful information on the water saturation could be ascertained. The reason for the 3-phase saturation errors has been ascribed to inaccuracies in the calculated calibrations due to what is believed to be beam hardening effects (preferential absorption of low energy X-rays). This instigated a study to quantify and correct for the effects of beam hardening in 3-phase measurements [6] which has led to a method to optimise tests with respect to X-ray energy and dopant selection to maximise the saturation accuracy, and supersedes the method described by Figure 3.

RELATIVE PERMEABILITIES

The condensate drainage relative permeability was deduced from the saturation measurements using a technique previously described for oil drainage studies [7]. Briefly, this is done as follows. First, the oil flow velocity at a number of points along

the core is calculated from the saturation changes above that point. Secondly, the condensate permeability is calculated for the saturation at each point from that rate, assuming the flow is driven by the gravity head due to differences in oil and gas densities. This neglects the capillary pressure gradient and so in this case the method could not be applied to the bottom section of the core which was shown to be end effected (Figure 5). Generally the end effect would be expected to be small at the low gas/oil IFTs exhibited by condensate fluids. Data quality was affected by the operational problems with this new facility described earlier, but using in-situ saturation data from scans after 6 days of drainage, the most unfavourable interpretation is a condensate relative permeability of 0.0003 at an oil saturation of 9%PV. Fitting this value to the Corey form used in the simulation studies (Equation (1)) yields a Corey exponent, n_o , of 4.

This relative permeability was two orders of magnitude higher than that deduced for low pressure gas/oil gravity drainage experiments on similar core material. This could be because of the much lower interfacial tension and/or the method in which the oil saturation is produced. We estimate the gas/oil IFT for this experiment to be 0.44 mN/m and the Bond number to be about 6.5×10^{-6} . Field applicability may be questioned because of the relatively high connate water saturation, however, the conditions were more representative than those in the experiments described earlier.

SIMULATION STUDY

The simulation study was performed using two basic simulation models. The first was a simple 1D column, which looked at the effects of vertical permeability, condensate PVT, and oil relative permeability on liquid drainage. The second was a 2D model representing a dipping reservoir, which looked at additional parameters involving horizontal as well as vertical movement of liquid. In some cases the 2D model was modified to include an explicit shale representation.

Grid Data

Both models represented a reservoir unit 100 m thick and of area 1 km by 1 km. The 1D model was subdivided into 50 equal layers. The 2D model dipped at a constant 20 degrees. Usually it was uniformly split into 20 blocks in the x-direction and 20 layers in the z-direction, but additional refinement was introduced for certain of the cases involving shales, as described below. The models had a constant porosity of 20%. Rock permeability was varied over the range 10 to 1000 md, both horizontally and vertically.

PVT Data

Two condensates were modelled. These were chosen so that drainage could be studied for both medium and rich gas condensates. The model liquid saturation developments under constant volume depletion are shown in Figure 8, with maximum condensate saturations of about 21% and 34% for the medium and rich fluids, respectively.

Calculated gas/oil IFTs and Bond numbers for 1000 md rock are given in Figure 9, excluding a small range just below the dewpoint pressure. IFTs for the rich condensate are lower than those for the medium condensate in the high-pressure region because the former is closer to critical. If the critical Bond number for enhancement of k_{ro} was 1×10^{-4} , then any assistance to gravity drainage would be short lived. If it was 1×10^{-5} , then enhanced drainage could be operative for several years.

Relative Permeabilities

The intention of this project was to examine the potential for condensate drainage so the aqueous phase in the simulation models was set to be immobile at a connate saturation of 0.2. Because of the uncertainty over the condensate relative permeability curve, oil and gas relative permeability curves were obtained from Corey expressions as follows,

$$k_{rog} = \left[\frac{(S_o - S_{org})}{(1 - S_{wc} - S_{org})} \right]^{n_o} \quad (1)$$

$$k_{rg} = \left[\frac{(S_g - S_{gr})}{(1 - S_{wc} - S_{gr})} \right]^{n_g} \quad (2)$$

and the oil Corey exponent, n_o , was varied over the likely range (3 and higher).

Example k_{ro} curves, for $n_o=3$ and $n_o=6$, are shown in Figure 10. The ultimate residual oil saturation is zero in both cases but the curve for $n_o=3$ is much more favourable to drainage, particularly for low condensate saturations.

There is a number of factors to consider in trying to deduce appropriate k_{ro} curves from the laboratory results. For example, in the 2D simulation models condensate can flow both vertically and along the dip. These directions will have different Bond numbers and thus, possibly, different values for k_{ro} . However, in the models used here, flow along the dip is, at least for some cases, most important when condensate has collected at some barrier to vertical flow. The condensate saturation will then be high and the choice of k_{ro} curve will be of little significance. In evaluating k_{ro} for vertical flow, one must also consider the appropriate level of vertical permeability with which to determine the Bond number and the effect of heterogeneities which are not resolved in coarse-grid models.

Well Data

In both models, depletion normally occurred via a producer completed in a single block, with a gas production rate constraint equivalent to 7.5% GIIP per annum, and a minimum BHP constraint of 1000 psi.

Initialisation

Both models were initialised with single-phase gas condensate, at around 200 psi above the dewpoint pressure, in the presence

of connate water. There was no underlying aquifer. Most cases were run for 10 years of production.

1D SIMULATION

A list of the cases run using the 1D simulation model is shown in Table 3 together the thickness of the oil column at the base of the reservoir for each case at the end of the simulation. We use this thickness to characterise the results of the sensitivity studies.

Base Case

The base case used the medium condensate, with a favourable vertical permeability of 1000 md, and a favourable oil Corey exponent, n_o , of 3. The liquid drains rapidly to the base of the model to form a column about 24 m thick at end of field life. This result shows that under favourable circumstances significant drainage of oil is possible at the field scale.

The calculated gas/oil IFT increases with time, and also increases slightly with depth (Figure 11). The variation with depth shows that the composition of the phases varies with depth, and demonstrates the desirability of compositional simulation, rather than use of an extended black-oil model. Typical Bond numbers for this 1000 md example decrease gradually over time from 2.3×10^{-5} at 1 year of production, to 7.8×10^{-6} at 3 years, and 2.3×10^{-6} at 7 years. Thus beneficial Bond number effects on k_{ro} may assist drainage for almost three years of production if the critical Bond number is 1×10^{-5} .

2D SIMULATION

A list of the cases run using the 2D simulation models, together with the height of the oil column at the base of the reservoir at the end of the simulation for each case, is shown in Table 4. This thickness may be used to help characterise the results of the sensitivity studies.

Base Case

Figure 12 shows liquid saturation profiles with increasing periods of production for the base case which used the medium condensate with favourable rock properties of $n_o=3$ and $k_v=k_h=1000$ md. The condensate liquid drains to the bottom of the sand, where it forms a thin layer and then migrates down-dip to form a column at the base of the reservoir. The oil layer has a thickness of only 1 gridblock (5 m) so that the oil saturation, and thus its mobility, might be underestimated due to numerical dispersion. In this example, the final oil column has a maximum thickness of 120 m, demonstrating the possibility of significant oil drainage under favourable conditions.

Effect of Permeability

Liquid drainage in a dipping reservoir involves a component of flow along the sand, which becomes more important the greater the permeability anisotropy. With the 20° dip of this model the drainage flow rates in the two directions, in the absence of flow barriers and for a given oil saturation, are related by $u_v/u_h = 2.9 \times k_v/k_h$, so that down-dip flow exceeds the vertical flow for $k_v/k_h < 0.34$. Sensitivity to k_v was examined by reducing it from 1000 md to 100 md, and then to 10 md. Figure 13 shows the liquid saturation profile for the 10 md case. An oil layer does

not form on the base of the sand but a saturation front can be seen, extending up the reservoir, and, despite the lower vertical permeability, an appreciable oil column does form.

When the horizontal and vertical permeabilities are both low (10 md), liquid drainage is prevented (Table 4).

Effect of Condensate PVT

Sensitivity to condensate richness was examined by comparison simulations with the rich fluid. For $k_h=1000$ md, condensate drainage was significantly greater over the range of k_v examined (10 to 1000 md), with the final oil column being almost twice as thick as for the corresponding medium condensate case (Table 4).

Effect of Oil Relative Permeability

The oil relative permeability has a similar effect as that seen in the 1D models, with higher values of n_o causing significant reductions in liquid drainage (Table 4). Again, the sensitivity was reduced for the richer fluid.

Effect of Vertical Shales

In many fields, the vertical flow is not impeded by inherent permeability anisotropy, but by distinct sets of horizontal interbedded shales. These shales may be thin and not laterally continuous, so fluid may drain through intervening gasps. In a dipping reservoir shales might assist condensate drainage since condensate would only have to drain a relatively short distance before it met its first shale. Condensate could collect on this shale, raising the local saturation, and, from then on, condensate could travel at a high value of k_{ro} . This might be particularly effective in situations where there are low IFTs in the initial stages of the depletion since condensate would have reached high saturations locally before the increase in IFT reduced the k_{ro} curve.

Shales such as this were modelled using vertical transmissibility barriers. The shales were modelled as occupying certain planes with a 15 m (that is, 3 gridblocks) vertical separation, and were 200 m long with 100 m gaps. The gaps of each layer of shales were offset against those above and below in a 'brick' pattern. Figure 14 shows these shales on the more refined grid described later in this section.

Simulation results using the medium fluid showed that the shales had little effect when rock properties were favourable to gravity drainage, but that the shales had an increasingly negative impact as rock properties were worsened (Table 4). The negative effects may well have been overestimated by numerical dispersion effects which reduce the oil saturation immediately above the shales and distort the flow of oil off the end of each shale. Also, there is a case to use a higher rock k_v in the cases with shales, since the reduced values of k_v used in models without explicit shale representations is partly to account for the effects of the shales. Single phase flow calculations for a case with $k_h=100$ md and $k_v=10$ md showed the overall vertical permeability was reduced to 1 md by the shales.

To reduce the effects of numerical dispersion, the simulation model was slightly modified to give better resolution. Gridblock

thickness was reduced from 5 to 2 m in those layers immediately above shales to give better predictions of oil saturations immediately above shales. Gridblock size was halved in the x-direction to give a better description of flow off the end of the shales. (These changes were found to slightly increase the oil recovery from models containing shales compared with corresponding models without shales.) Also, the rich fluid was used and, to better model field practice, wells were completed over the full reservoir section. A wide range of oil relative permeabilities ($n_o=3$ and $n_o=6$) was examined using fairly pessimistic rock permeabilities ($k_h=100$ md, $k_v=10$ md). Resulting condensate saturations for up-dip production with $n_o=3$ are shown in Figure 15. With shales present, high condensate saturations develop on the shales and the region of low condensate saturation is more extensive. However, gross drainage is significantly reduced. Similar trends, with much reduced magnitude, are also seen with the less favourable oil relative permeability given by $n_o=6$ (Figure 16).

Recovery of Drained Liquid

The medium fluid with favourable assumptions on absolute and relative permeability ($k_v=k_h=1000$ md and $n_o=3$) showed appreciable gravity drainage (Figure 12). Two further simulations were performed which included production from the oil column in an attempt to improve oil recovery. In one case the production well was moved from the top of the reservoir to the base of the formation at the down-dip location. In the second the production well was similarly repositioned after 6 years of production from the crestal location. Both cases gave a doubling of the oil recovery (Figure 17), showing the potential benefits of gravity drainage in reservoirs with very favourable permeabilities.

Further cases were run to examine the benefits under conditions of less favourable rock permeability, corresponding to one of the rich fluid cases described above, namely $k_h=100$ md, $k_v=10$ md, with and without explicit shales. In these cases the down-dip producer was a vertical well at the extremity of the model and completed over the full formation. Predicted oil production curves for cases with $n_o=3$ are shown in Figure 18. These show a large (60%) benefit from the use of down-dip wells, with shales being beneficial to oil recovery for either production strategy. With $n_o=6$, the same trends are seen but to a much reduced extent (Figure 19).

DISCUSSION

Laboratory results have demonstrated that, in favourable circumstances, condensate may drain over a distance of 1 m over about 10 days. Scaling this to field timescale of 10 years would allow vertical drainage over a distance of almost 400 m. There is thus the potential for significant vertical drainage even when conditions are less favourable than those in the laboratory measurement. Furthermore, in many cases oil might collect at a barrier to vertical flow and then flow down-dip at a high oil saturation, providing a more favourable oil relative permeability.

The results from the simulation study reported above have confirmed the potential for condensate drainage under favourable circumstances, highlighting the importance of the condensate saturation, rock permeability, and condensate relative permeability (and thus, possibly, gas/oil IFT).

Recognising the simplicity of the models used in the simulation study, we may consider other evidence for the possible importance of gravity drainage, the most relevant being the many studies performed on recovery of waterflood residual oil through crestal gas injection, giving gravity drainage of oil in the presence of gas. Several field appraisals have identified the potential for technical success.

An advantage in making use of gravity drainage in condensate reservoirs is that there may be little or no additional costs compared to a standard development, it only being necessary to drill producers in suitable locations to capture drained oil rather than place them at the crest. For reservoirs under production, additional costs would be incurred by the need to drill suitably positioned wells, but these are small compared to the costs of a gas injection project. These factors suggest that improved oil recovery is likely to be feasible in some condensate reservoirs. Use of down-dip producers would also take advantage of any compositional gradients which may be present, in which the richness of a gas condensate often increases with depth. This possibility is limited, however, if the reservoir might be subject to significant aquifer influx.

Even when condensate drainage is not sufficient to allow improved liquids recovery through the use of down-dip wells, there may well be significant segregation locally. This might have implications for the success of other IOR schemes such as gas recycle below the dewpoint.

CONCLUSIONS

Published laboratory measurements of condensate relative permeability suggest it may be favourable for gravity drainage. A condensate drainage experiment performed with X-ray in-situ saturation measurements showed condensate liquid buildup at the outlet core face under the action of gravity and a reduction in this saturation on gas flooding.

A number of improvements to the X-ray saturation monitoring technique have been identified regarding calibration and normalisation for condensate and general coreflooding experiments the main points being:

- methane should not be used for gas calibration
- PVT tests to be performed before calibration
- use of Beam Hardening software for test optimisation
- ensure the full width of the core can be analysed.

The experiment showed that drainage can occur over distances of 1 m in only 10 days, demonstrating the scope for significant drainage within the time-scale of field developments.

Relative permeabilities were two orders of magnitude higher at low saturation than those deduced from low pressure gravity drainage experiments using conventional fluids, possibly because of reduced IFT.

A series of simulations performed using simple field-scale models support the possibility of significant condensate drainage occurring during the production of gas condensate reservoirs by natural depletion

The simulation results show that the development of a large oil column through condensate drainage is favoured by having a

rich condensate, high vertical and horizontal permeability, and a significant condensate relative permeability at low condensate saturation. The presence of discontinuous shales may also be beneficial.

In simple simulation models drained condensate can be captured using a suitably placed producer, raising the possibility of improved liquids recovery at little or no additional costs.

Even when gravity drainage is not sufficient to benefit condensate recovery, the more localised segregation may have implications for other IOR options, for example, gas recycling below the dewpoint.

Further work is required to better quantify the condensate relative permeability and to use more detailed models of fluid flow.

ACKNOWLEDGEMENT

This work was supported by the UK Department of Trade and Industry as part of its IOR studies at AEA Technology. The DTI's permission to publish is gratefully acknowledged.

REFERENCES

- [1] Danesh, A., Henderson, G.D., and Peden, J.M.: "Experimental Investigation of Critical Condensate saturation and its Dependence on Connate Water Saturation in Water-Wet Rocks," SPE 19695, presented at the 1989 Annual Fall Meeting of the SPE, San Antonio, TX, October 8-11.
- [2] Danesh, A. et al.: "Gas Condensate Recovery Studies," DTI IOR Research Dissemination Seminar, London, June 22-23, 1994.
- [3] Danesh, A. et al.: "Gas-Condensate Phase and Flow Behaviour: Mechanisms and Applications," 16th International Workshop and Symposium of the IEA Collaborative Project on EOR, Chiba, Japan, October 1995.
- [4] Boom, W., et al.: "Experimental Evidence for Improved Condensate Mobility at Near-Wellbore Flow Conditions," SPE 30766, presented at the 1995 Annual Fall Meeting of the SPE, Dallas, October 22-25.
- [5] Boom, W., et al.: "On the Use of Model Experiments for Assessing Improved Gas-Condensate Mobility Under Near-Wellbore Flow Conditions," SPE 36714, presented at the 1996 Annual Fall Meeting of the SPE, Denver, October 6-9.
- [6] "Modelling of and Correction for Beam Hardening Effects" Internal Report 60164/REP/1, Burch, S. F. and Hawker, B. M., 1996.
- [7] Goodyear, S.G. and Jones, P.I.R.: "Relative Permeabilities for Gravity Stabilised Gas Injection," 13th International Workshop and Symposium of the IEA Collaborative Project on EOR, Banff, Canada, September 27-30, 1992.

component	mole percent
methane	80
ethane	11
n-butane	4
heptane	3
decane	1.4
dodecane	0.6

Table 1 Synthetic condensate composition

length	88.0cm
diameter	4.1cm
bulk volume	1161.8cm ³
pore volume	232.6cm ³
porosity	20.0%
absolute gas permeability	1124 mD
absolute brine permeability	762 mD
S_{wi}	32.1 %PV
N_2 permeability at S_{wi}	901 mD

Table 2. Core Characterisation Properties

Medium Condensate

	$k_v=1000$ md	$k_v=100$ md	$k_v=10$ md
$n_o=3$	24	20	2
$n_o=4$	18	10	0
$n_o=5$	12	4	0
$n_o=6$	6	2	
$n_o=8$	0	0	

Rich Condensate

	$k_v=1000$ md	$k_v=100$ md	$k_v=10$ md
$n_o=3$	40	38	6
$n_o=4$	36	30	2
$n_o=5$	30	20	0
$n_o=6$	26	10	
$n_o=8$	12	2	

Table 3 1D Results: Thickness of Final Oil Column (m) as a Function of Permeability and Oil Corey Exponent

Medium Condensate

k_h (md)	k_v (md)	n_o	Shales	Comments	Final oil column (m)
1000	1000	3	no	Fig. 12	120
1000	100	3	no		110
1000	10	3	no	Fig. 13	100
100	100	3	no		70
10	10	3	no		0
1000	1000	6	no		30
1000	1000	3	yes		120
1000	10	3	yes	GOC not horizontal	50-100
1000	1000	6	yes		0

Rich Condensate

k_h (md)	k_v (md)	n_o	Shales	Comments	Final oil column (m)
1000	1000	3	no		205
1000	100	3	no		200
1000	10	3	no		190
1000	1000	6	no		140
100	10	3	no	Refined grid, GOC not horizontal, Fig. 15	105-210
100	10	3	yes	Refined grid, GOC not horizontal, Fig. 15	105-170
100	10	6	no	Refined grid, Fig. 16	0
100	10	6	yes	Refined grid, Fig. 16	0

Table 4 2D Results: Thickness of Final Oil Column

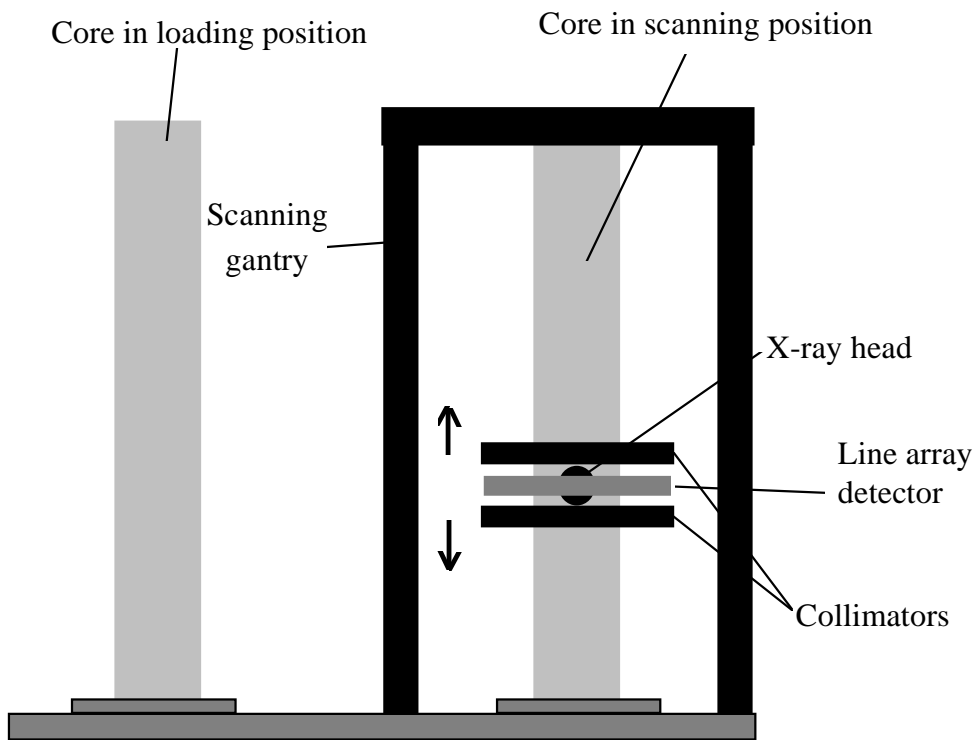


Figure 1: X-ray Scanning Platform: Schematic Side View

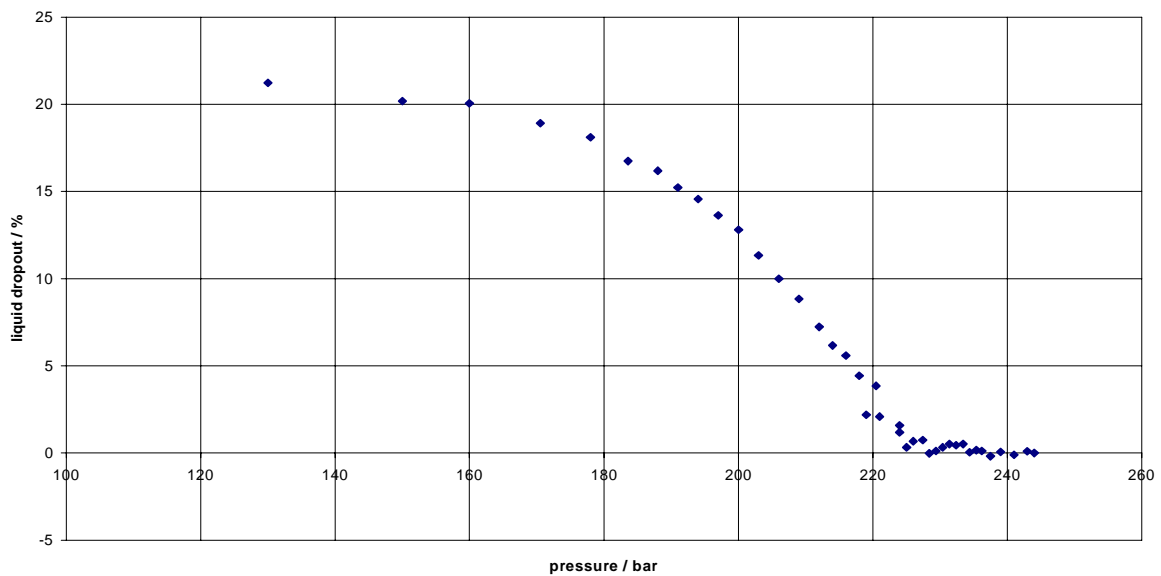


Figure 2 Synthetic 6 component condensate CCE

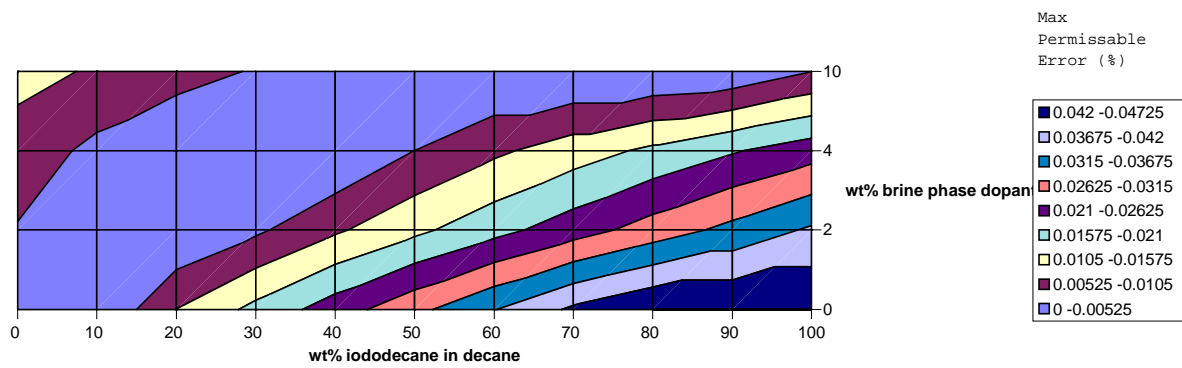


Figure 3 Effect of oil and brine phase dopants on maximum permissible scanning error to give +/- 1% error in S_o

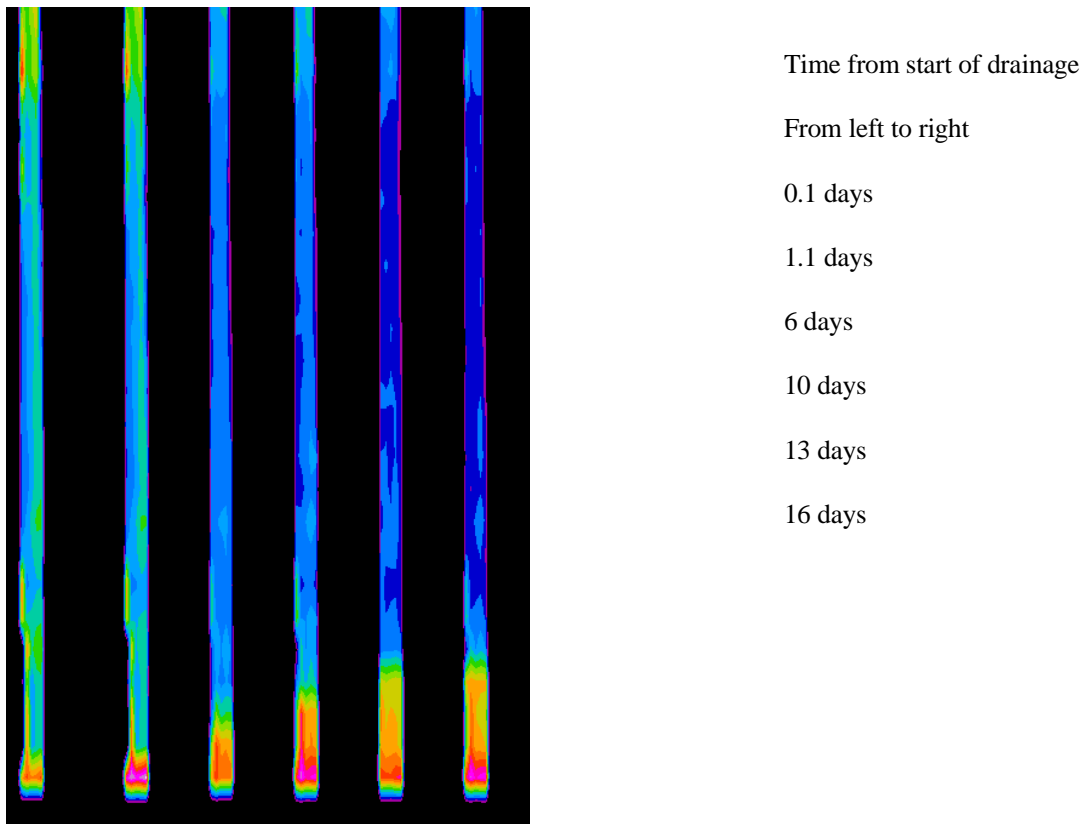


Figure 4: Qualitative Images of Condensate Drainage

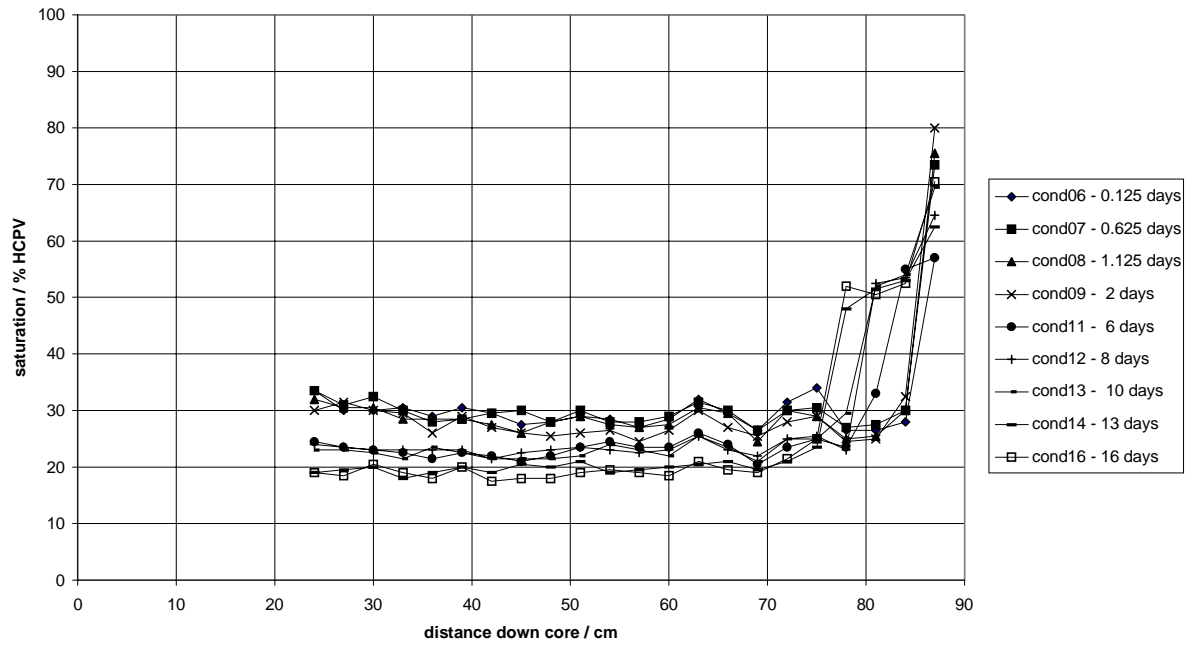


Figure 5 Liquid condensate saturation during drainage

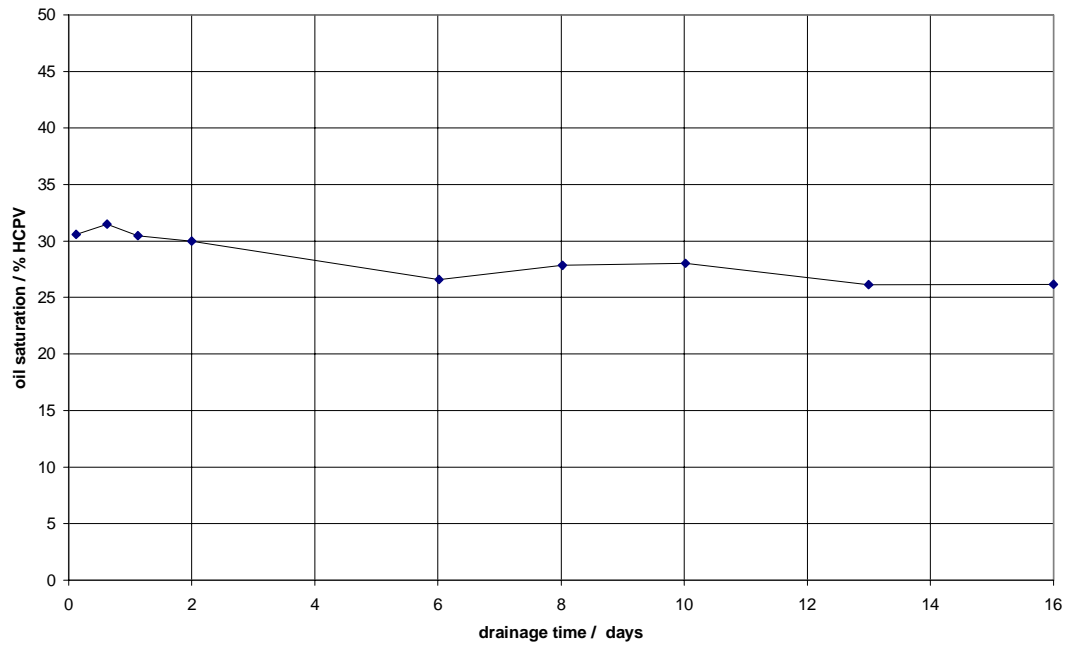


Figure 6. Average liquid condensate saturation during drainage

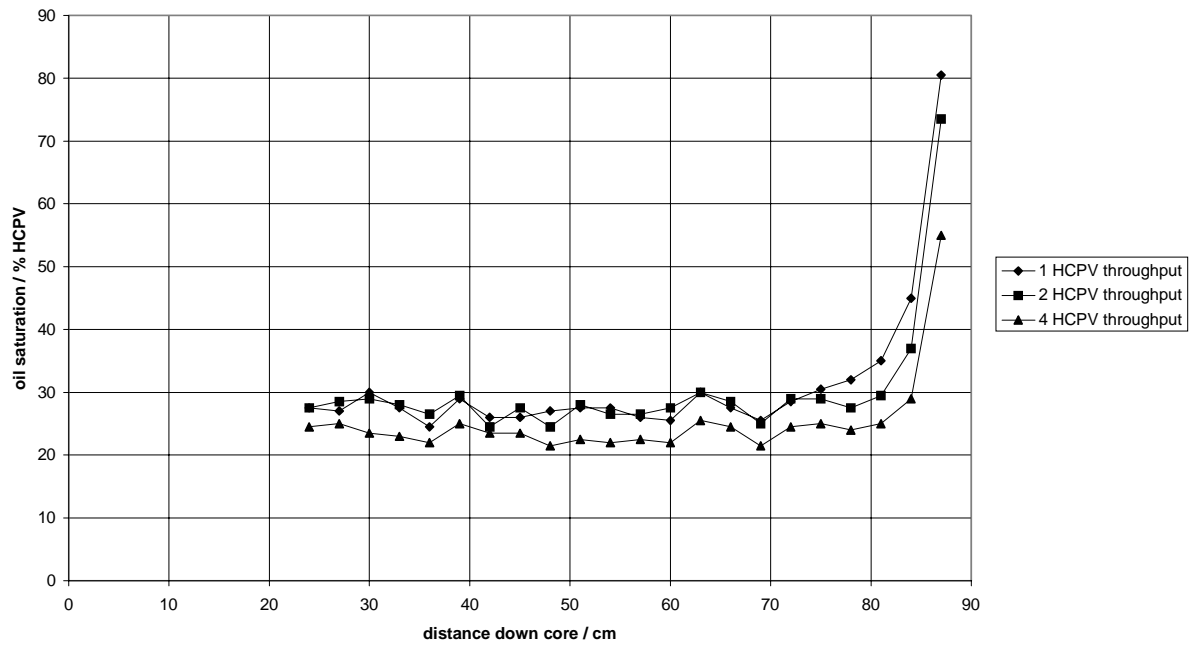


Figure 7 Liquid condensate saturation during gas flood

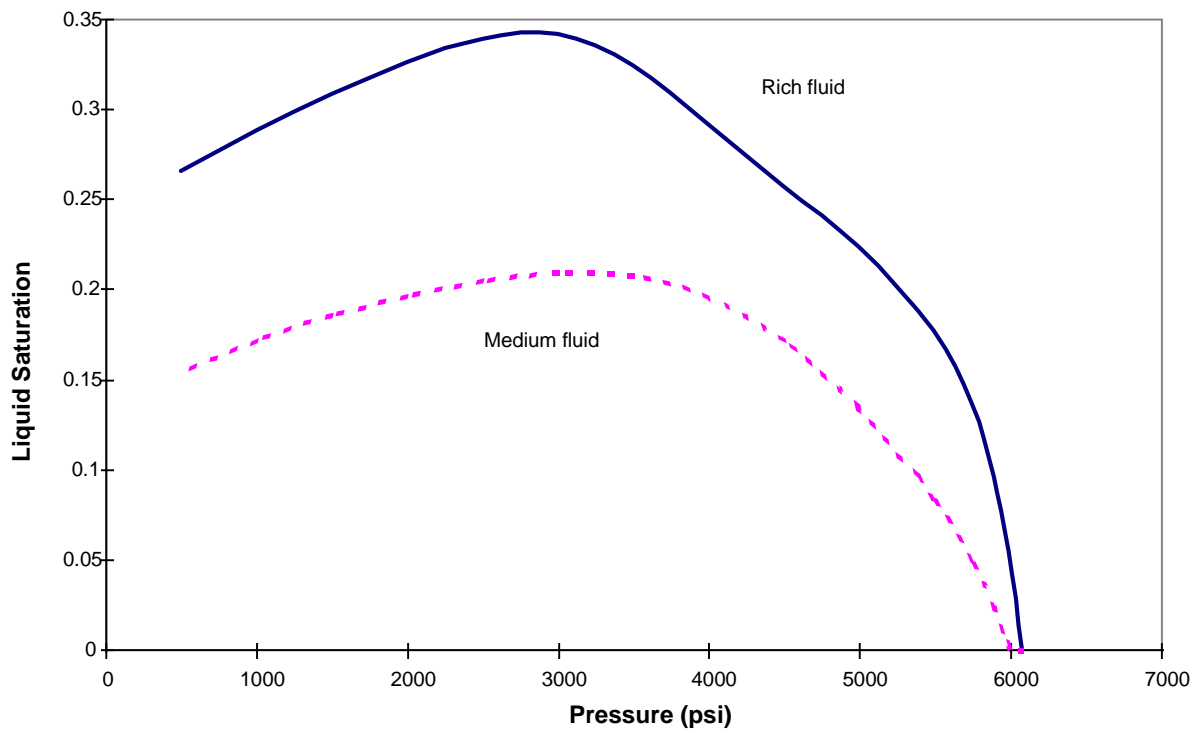


Figure 8: Liquid Dropout in Constant Volume Depletion

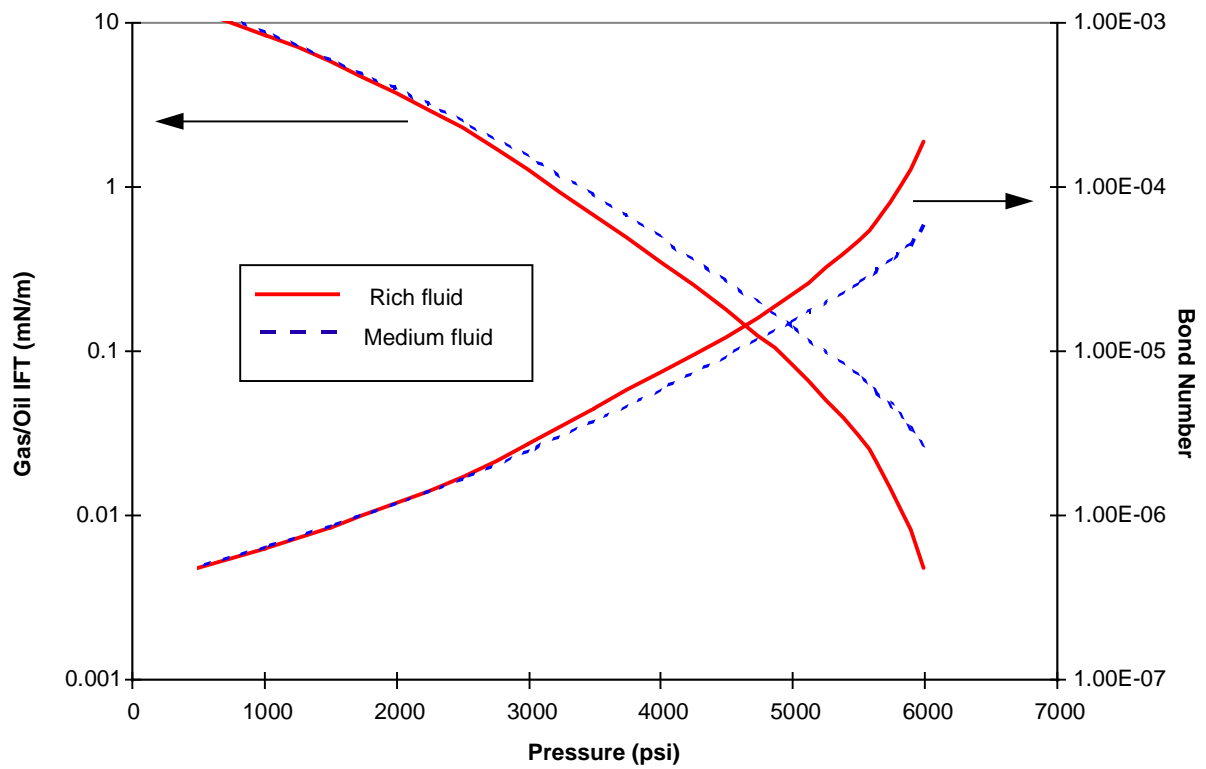


Figure 9: Gas/Oil IFT and Bond Number Prediction (1000 md rock)

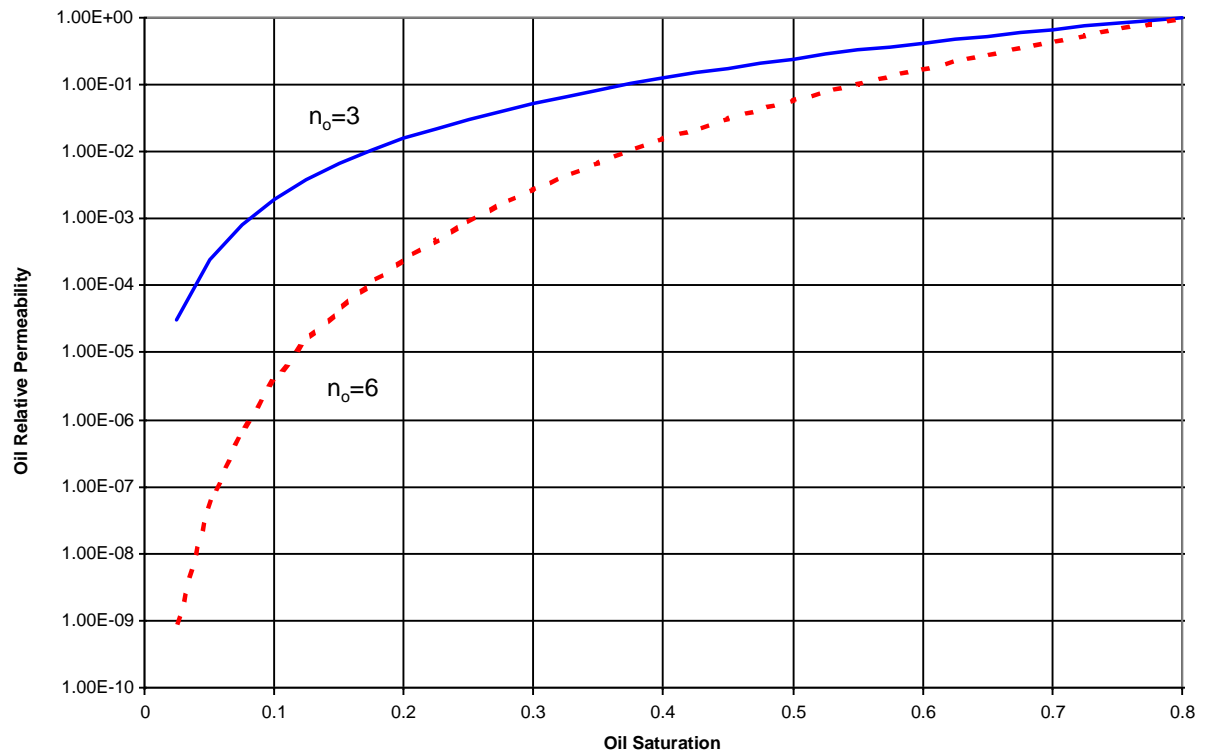


Figure 10: Example Oil Relative Permeability Curves ($n_o=3$ and $n_o=6$)

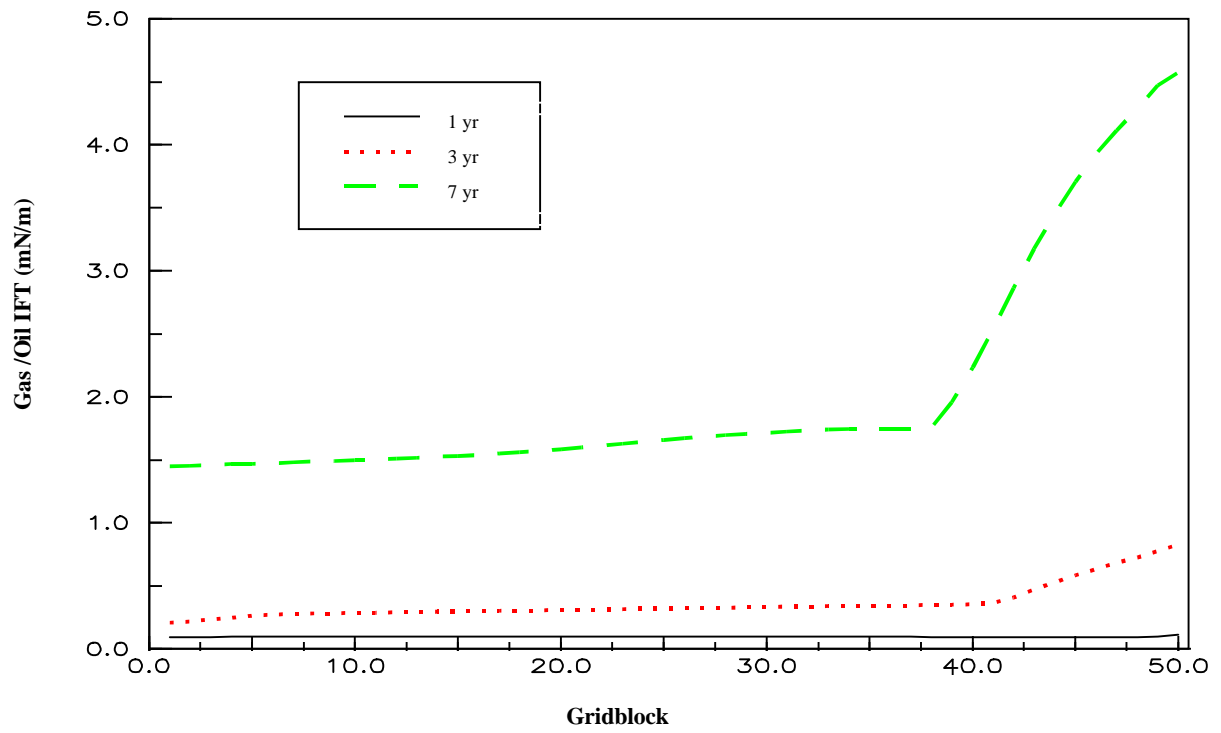


Figure 11: Variation of gas/oil IFT with time and position (Medium fluid, $K_v=1000\text{md}$)

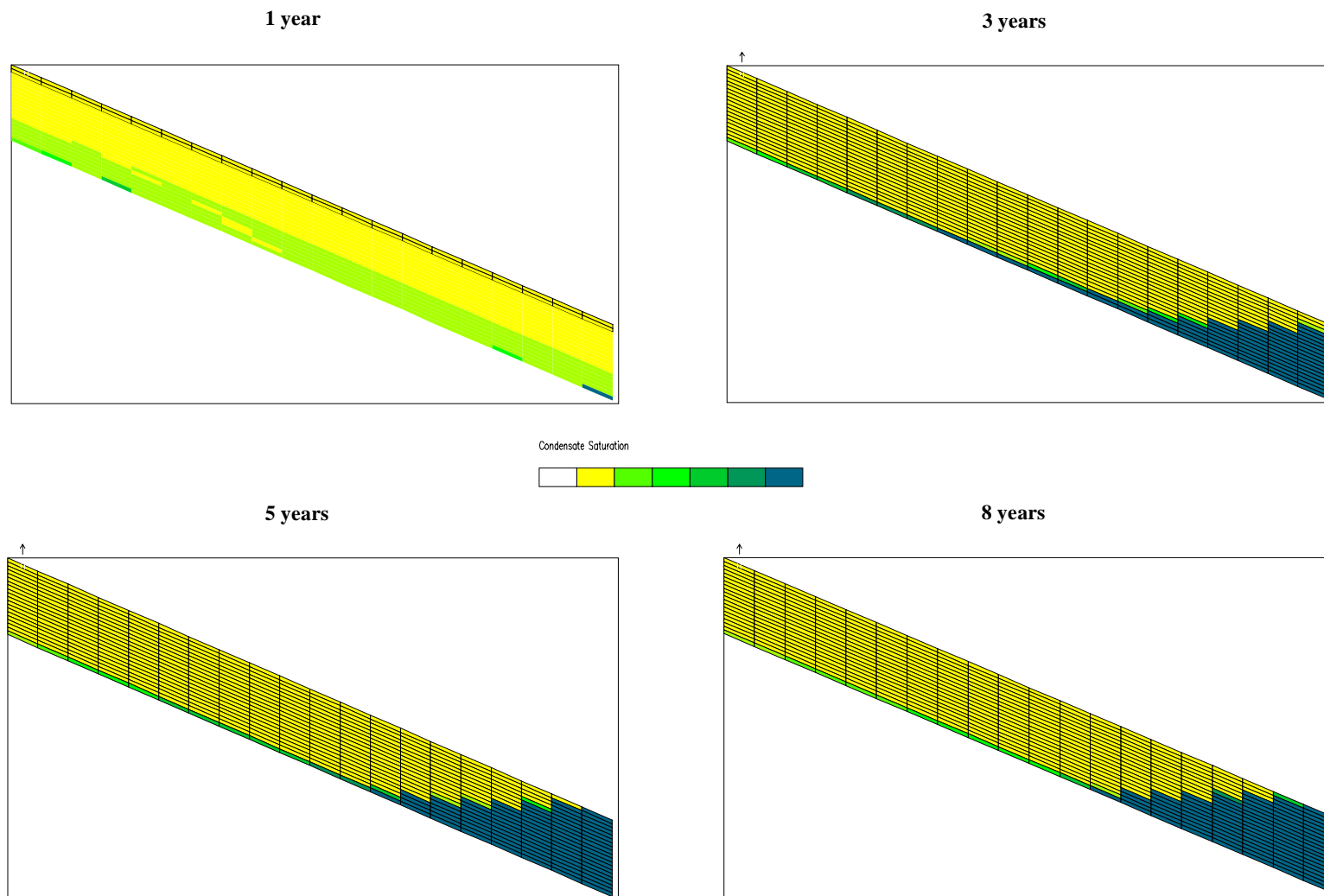


Figure 12: Condensate Drainage for 2D Base Case (Medium fluid, $k_h=k_v=1000$ md, $n_o=3$)

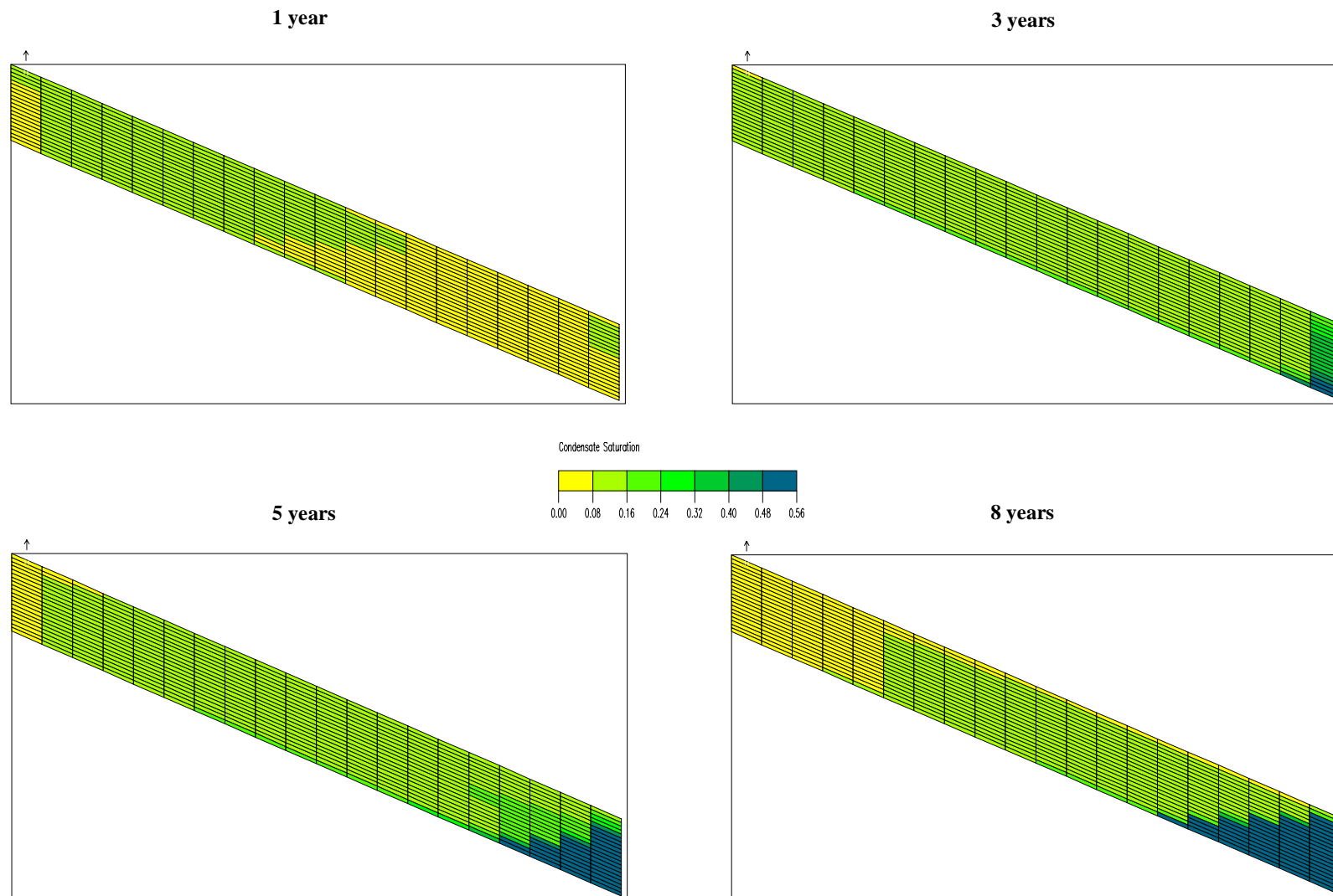


Figure 13: Condensate Drainage with $k_v=10$ md (Medium fluid, $k_h=1000$ md, $n_o=3$)

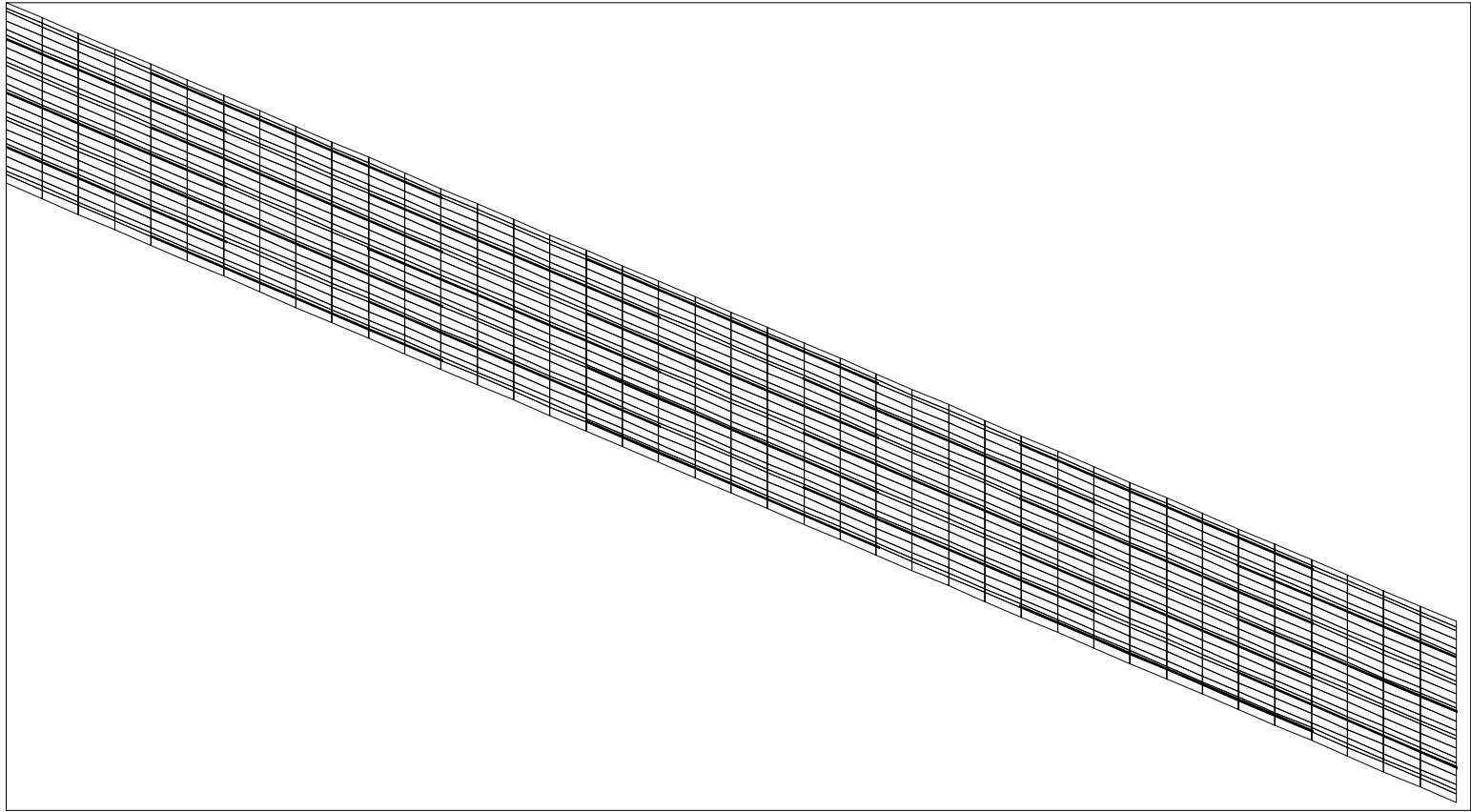
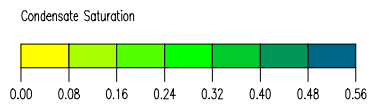
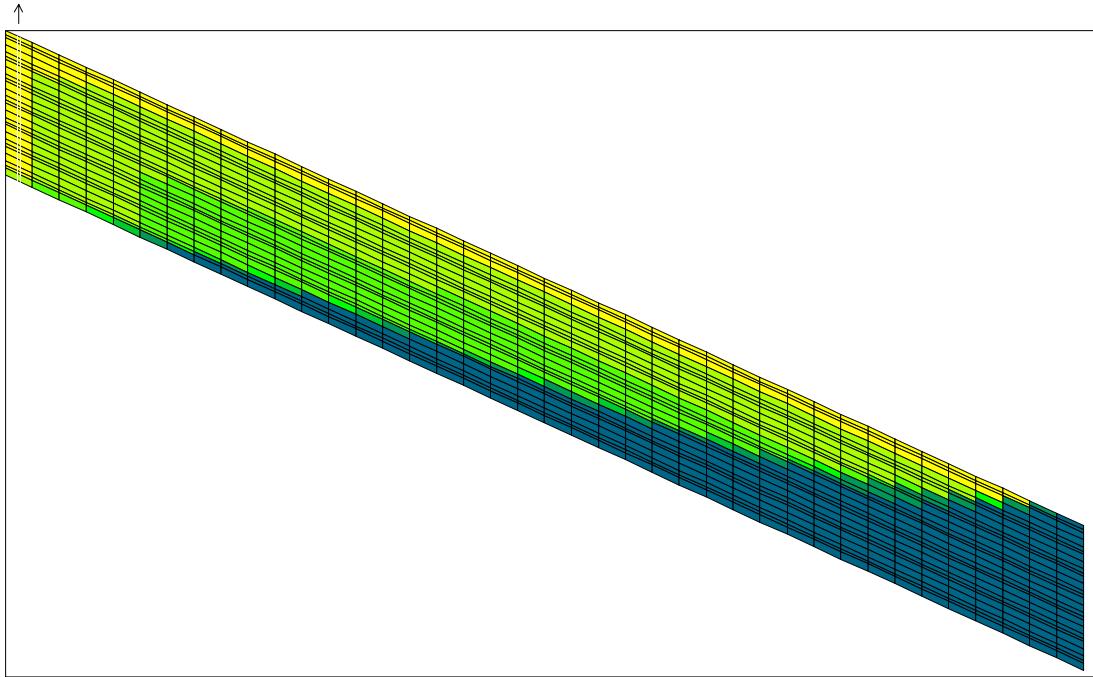


Figure 14: Shales on Refined Grid

Without Shales



With Shales

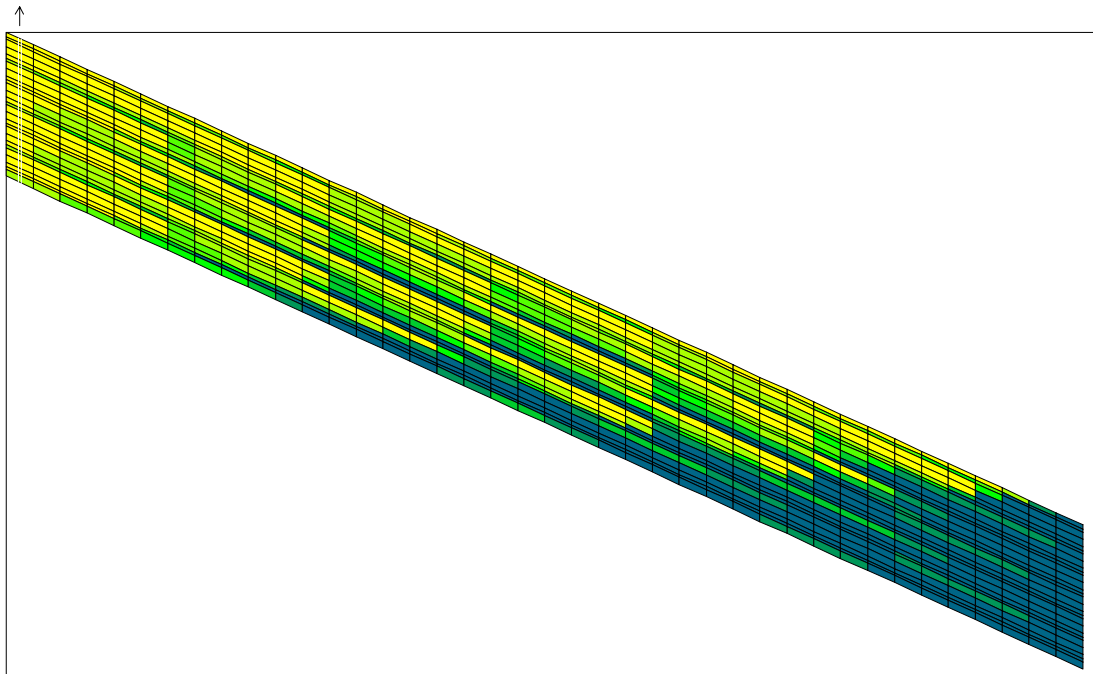


Figure 15 Sensitivity of Condensate Drainage to Shales
(Rich fluid, $k_h=100$ md, $k_v=10$ md, $n_o=3$)

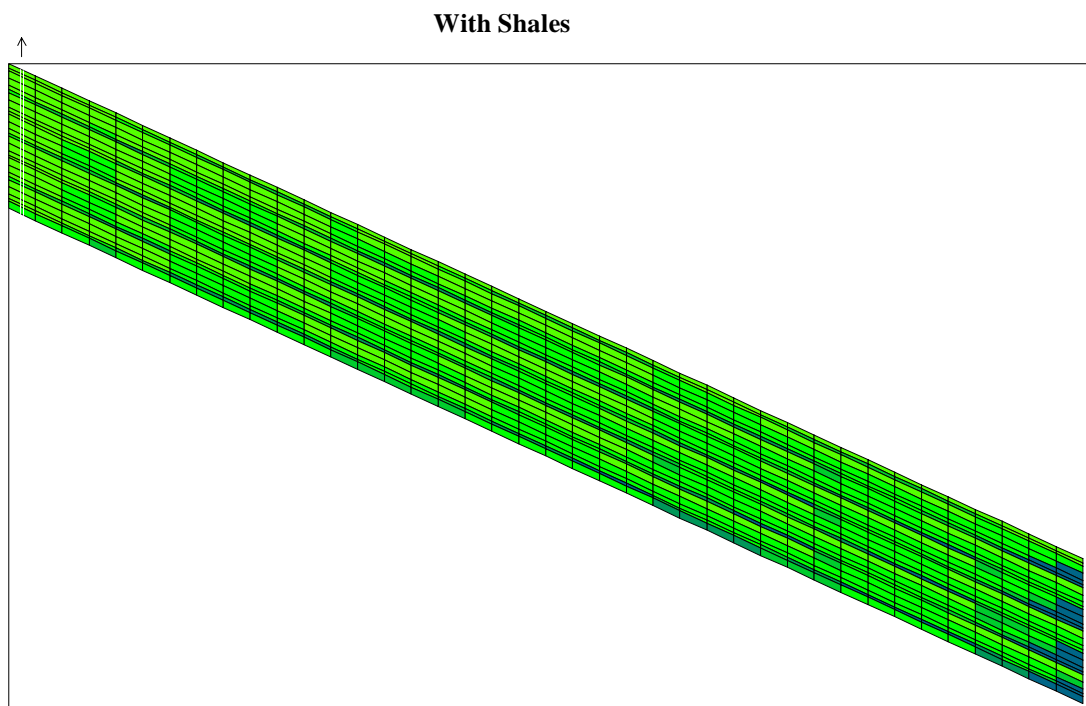
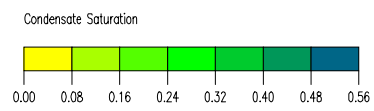
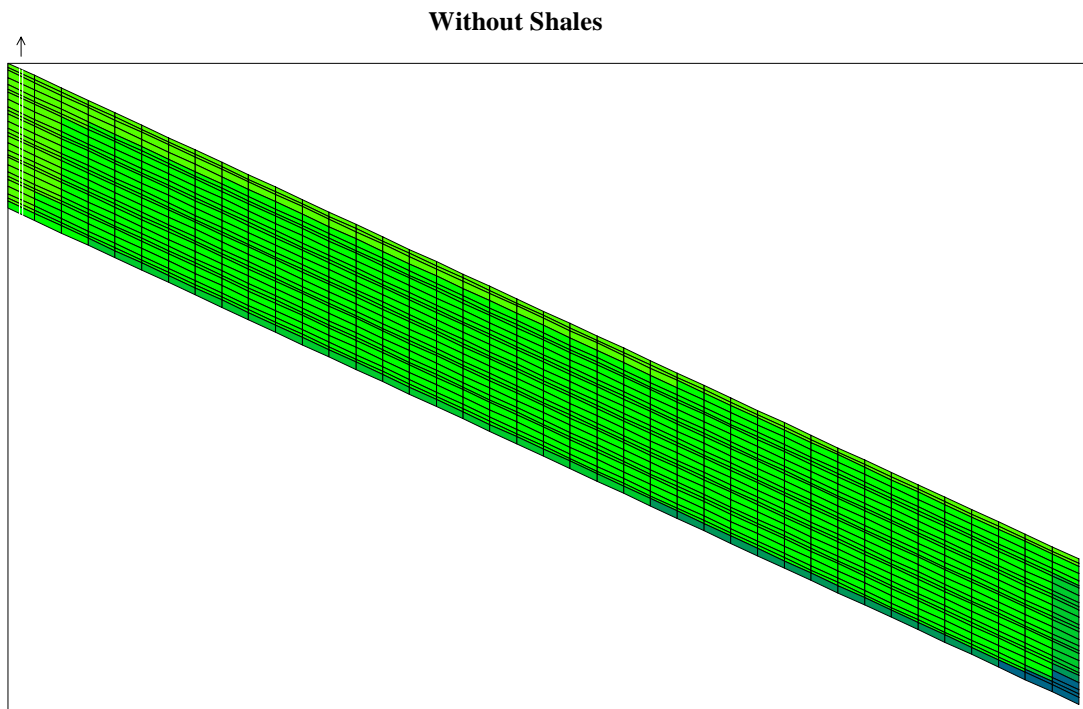


Figure 16: Sensitivity of Condensate Drainage to Shales
(Rich fluid, $k_h=100$ md, $k_v=10$ md, $n_o=6$)

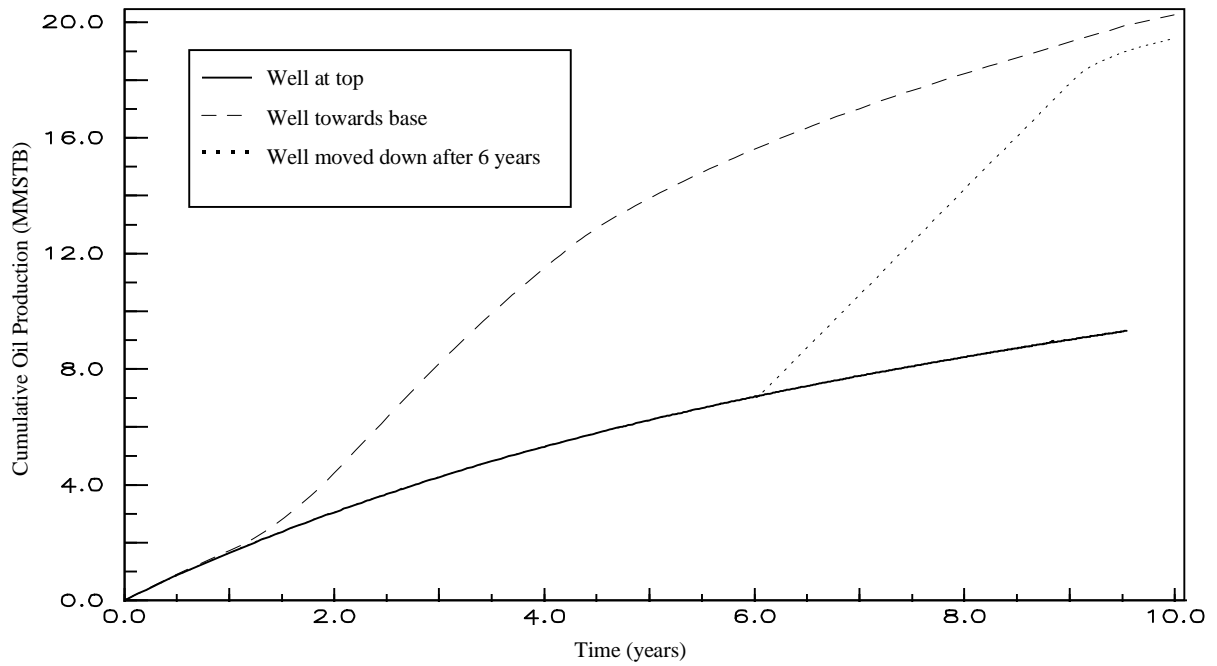


Figure 17: Oil Production Comparisons (Medium fluid, $k_v=k_h=1000$ md, $n_o=3$)

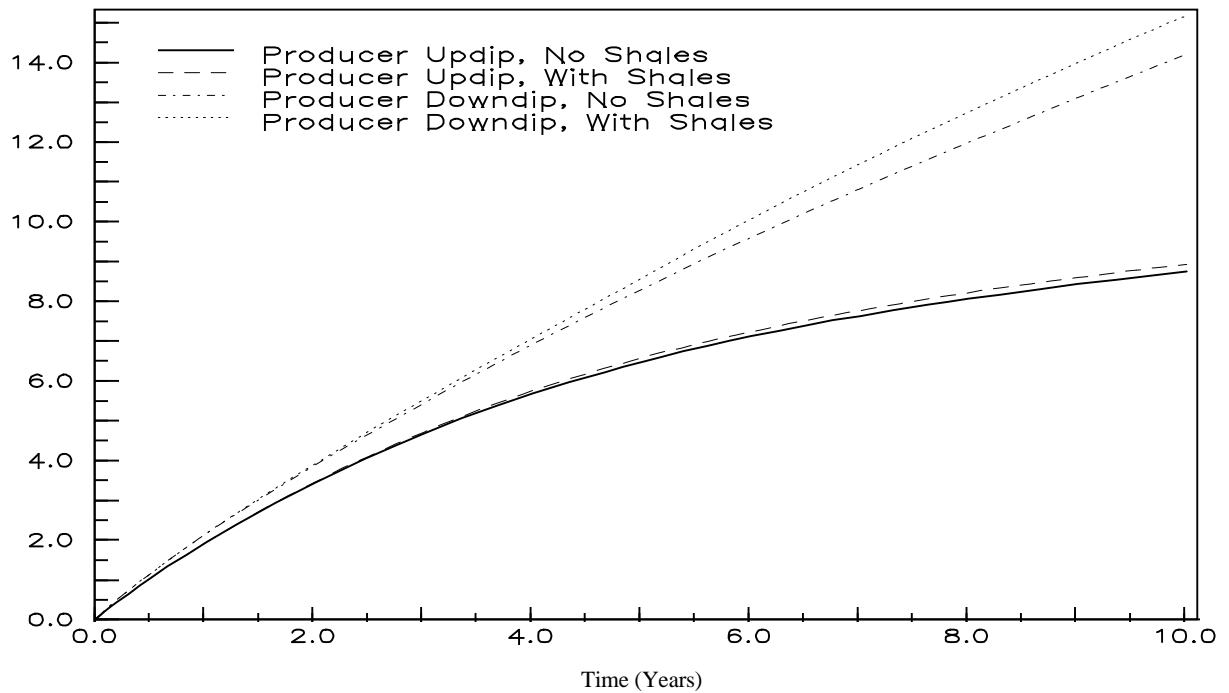


Figure 18: Oil Production Comparisons (Rich fluid, $k_h=100$ md, $k_v=10$ md, $n_o=3$)

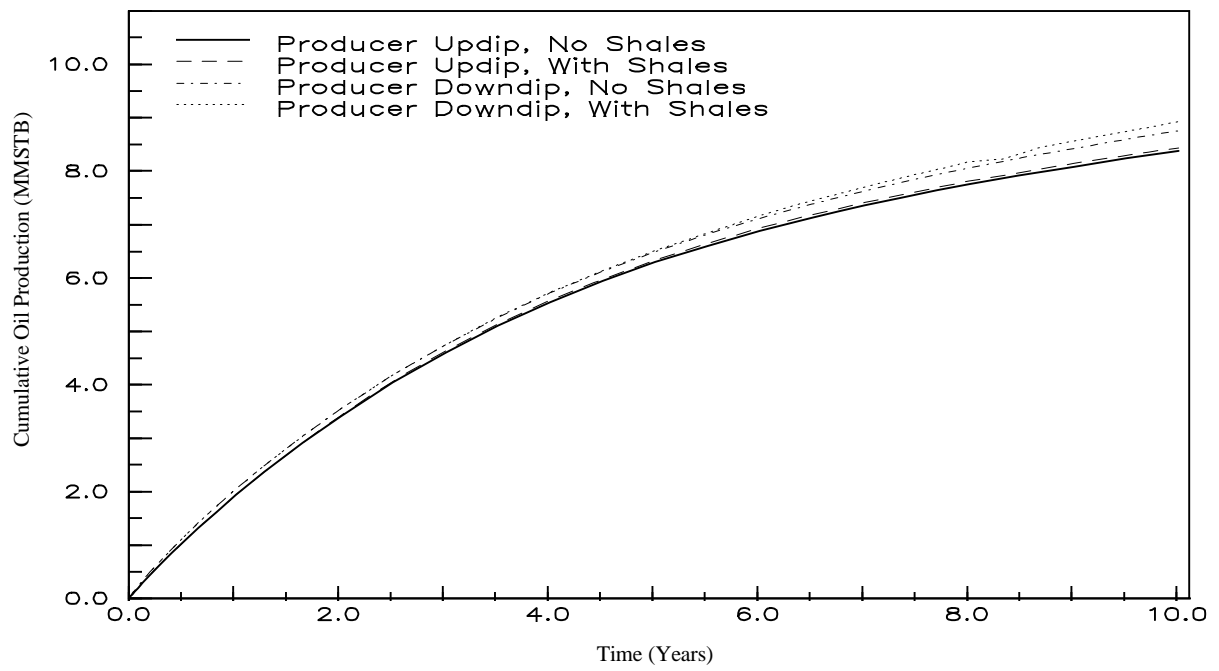


Figure 19: Oil Production Comparisons (Rich fluid, $k_h=100$ md, $k_v=10$ md, $n_o=6$)